Pak. J. Biochem. Mol. Biol. 2011; 44(1): 1-7

Prediction of enzyme-inhibitor interactions in *Avicennia marina* Cu-Zn superoxide dismutase: implications of functionally significant residues in the metal binding sites

Uzma Jabeen[1], Asmat Salim[2] and Atiya Abbasi[1]*
[1]HEJ Research Institute of Chemistry, [2]Dr. Panjwani Center for Molecular Medicine and Drug Research, International Center for Chemical and Biological Sciences, University, Karachi, Karachi, Pakistan

Abstract: 3D homology model of Cu-Zn superoxide dismutase from *Avicennia marina* (AMSOD) was constructed using the structural coordinates of Spinach SOD (SSOD). Structural features of the model were outlined and correlated with respective functional aspects. Despite the similar overall fold, the homology model of AMSOD showed some distinct structural changes as compared to the template, SSOD. AMSOD was also modeled with specific inhibitors; azide, phosphate, thiocyanide and nitrite. Despite sequence variations, the inhibitor-enzyme interactions were quite similar. We also report some changes in the structure of AMSOD after mutation (P108D and H109Y) at the crucial sites.

Keywords: Homology modeling, structure prediction, superoxide dismutase, *Avicennia marina*.
Received: December 22, 2010 **Accepted:** February 10, 2011
***Author for Correspondence:** asmat.salim@iccs.edu

INTRODUCTION

Plants in the environment are exposed to a range of abiotic stresses like osmotic, salinity, temperature and heavy metal toxicity which affect their growth and other physiological processes[1]. The metallo-enzyme, superoxide dismutase (SOD) plays a vital role in protecting aerobic organisms against oxidative damage and catalyzes the dismutation of superoxide radicals to H_2O_2 and molecular oxygen. These reactions are catalyzed by superoxide dismutases (SODs) that are divided into four groups according to their metal cofactor requirements. These are copper/zinc (Cu, Zn-SOD), manganese (MnSOD), iron (FeSOD) and NiSODs which are located in different compartments of the cell. NiSODs are present in prokaryotes[2]. In plants, under abiotic stress or even under optimal conditions, free radical reactions take place where active oxygen species (AOS) like superoxide, hydroxyl, alkoxyl radicals and hydrogen peroxide are produced as metabolic by-products in different subcellular compartments[3-5]. Cu, Zn-SOD is the most abundant enzyme and has been localized in the cytosol, peroxisome, chloroplast, and apoplast[4,5]. The enzymatic mechanism proposed for Cu, Zn-SOD is the reduction of oxidized Cu(II) form of the enzyme by superoxide releasing dioxygen, alternating with oxidation of the reduced Cu(I) form by another superoxide anion and two protons, generating hydrogen peroxide[6].

Mangroves are salt tolerant plants and show increased SOD activities when transferred from fresh water to high salinity[7]**.** Residue His63 and the Cu ion are essential for the dismutase reaction, while Zn appears to be essential for the dissociation of the hydrogen peroxide formed and for the pH stability of the reaction. The crystalloghraphic structure of Cu,Zn-SODs from human, spinach, yeast and *E.coli* have a flattened antiparallel β-barrel, composed of eight strands arranged in the Greek-key topological order. Thermochemical stability of SOD might be attributed to this eight-stranded β-barrel motif. Other factors include hydrophobic interactions (associated with dimerization that contributes to stability through the reduction of its mobility), coordinate covalent bonds, and an intra-subunit disulfide bond between highly conserved pair of cysteines[8]. It has been demonstrated that binding of small anions (azide, thiocyanate) at the catalytic site competitively inhibit the enzyme. This provides insight about the binding of superoxide anion to the copper ion at the catalytic site of Cu, Zn-SODs[9].

In the present study we constructed the 3D homology model of *Avicennia marina* superoxide dismutase (AMSOD) bound with Cu and Zn ions present at the catalytic site. AMSOD was also modeled with specific inhibitors, azide, phosphate, thiocyanide and nitrite. The structural information obtained from the model was compared with those of the reported crystal structures. We have also done some mutational studies at the crucial sites in the structure and predicted the changes that follow.

MATERIALS AND METHODS

Sequence analysis

Primary amino acid sequence of AMSOD was retrieved from the SWISSPORT data bank[10]. The sequence was submitted to the BLAST server that searched for the appropriate template using Gapped BLAST and PSI-BLAST algorithms[11] against the sequences in the protein data bank, PDB[12]. The highest sequence homology was found to be 70% with spinach Cu,Zn-SOD (Pdb id: 1srd)[13].

Model building

The three-dimensional homology model of AMSOD with Cu and Zn ions was built using the structural coordinates of spinach Cu,Zn-SOD (Pdb id: 1srd) [13] by the protein structure modeling program MODELLER9v3[14,15]. Separate homology models of AMSOD with azide, thiocyanide, nitrate and phosphate were built using the structural coordinates of bovine superoxide dismutase bound with azide (pdb id: 1sxz-B), bovine superoxide dismutase bound with thiocyanide (pdb id: 1sxs-B) [9], bovine superoxide dismutase bound with peroxynitrite (pdb id: 1sda-G)[16] and yeast superoxide dismutase exposed to nitric oxide and phosphate (pdb id: 1f1g)[16,17] by MODELLER 9v3. The three dimensional (3D) coordinates of the templates were retrieved from PDB[12]. Protein structures were visualized and analyzed with SPDV viewer 3.7[18] and DS viewer[19].

Model assessment

Assessment of the predicted homology models was based on the analyses of geometry, stereochemistry and energy distributions in the model. The consistency of the predicted homology models were assessed using the ENERGY command of the MODELLER. Assessment was further conducted by programs PROCHECK[20] and ProSa[21, 22]. The variability among the models was compared by the superpositions of the Cα traces and backbones of the models onto the templates from where the RMSD values for positional differences between the equivalent atoms could be determined. Hydrogen-bonding, molecular surface accessibility, protein-cofactor contacts and ion pairs were calculated by the program WHATIF[23].

Mutation prediction

Mutation prediction was carried out in the predicted 3D homology model of AMSOD by using SPDV viewer (3.7). Pro108 to Asp and His109 to Tyr mutations were performed in the homology model of nitrite bound AMSOD.

RESULTS AND DISCUSSION

Unbound AMSOD model

The homology model of unbound Cu, Zn-superoxide dismutase from *Avicennia marina* (AMSOD) was built using the 3D structural coordinates of spinach superoxide dismutase (Pdb id: 1srd) as the template. AMSOD closely resembles the structure of 1srd (Table 1). The position of the functionally important residues in the structure is retained in the model when compared with the other Cu, Zn SODs and the overall packing of the flattened Greek-key nine-stranded beta-barrel is maintained (Figure 1). The ProSA energy plot shows the local model quality by plotting energies as a function of amino acid sequence position**.** In case of the homology models of AMSOD, ProSA analysis revealed Z-scores which lie in the low energy conformation states.

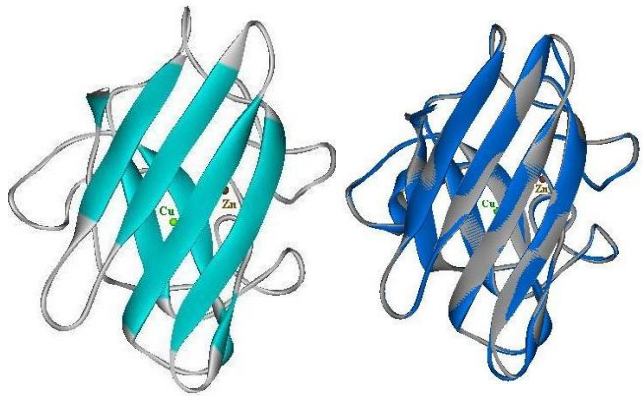

a) ***b)***

Figure 1: (a) The 3D Homology Model *A. marina* superoxide dismutase showing the secondary structural features showing the Cu and Zn ions (b) Superposition of superoxide dismutase from *A. marina* (grey) and Spinach peroxidase (blue).

Table 1: Details of the homology models of *Avicennia marina* superoxide dismutase

Models	Templates	Procheck statistics	r.m.s.d. (Å)
Unbound Model	Spinach cu,zn-SOD (1srd)	95.6% residues fall in the most favored region 4.4% in the allowed regions	0.32Å
Azide Bound Model	Bovine cu,zn- SOD (1sxz)	91% residues fall in the most favored 9% in the allowed region	0.32Å
Thiocyanide Bound Model	Bovine cu,zn- SOD (1sxs)	93.0% residues fall in the most favored region 7.0% in the allowed region	0.33Å
Nitrite Bound Model	Bovine cu,zn- SOD (1sda)	90.4% residues fall in the most favored region 9.6% in the allowed region	0.28Å
Phosphate Bound Model	Yeast cu,zn -SOD (1fig)	92.1.0% residues fall in the most favored region 7.9% residues in the allowed region	0.38Å

Active site geometry

The metal-binding site of Cu, Zn-SOD is highly conserved. The active site is situated at the base of a superficial channel formed by two loops extending from the β-barrel. The Cu is coordinated with nitrogen provided by side chains of histidines at positions, 45, 47, 62 and 119 and exhibits a compressed tetrahedral geometry. The interaction between these active site residues in the form of

hydrogen bonds and salt bridges is outlined in Table 2. The interaction is largely conserved with a few alterations due to changes in the sequence or orientation of the amino acids. Multiple sequence alignment by CLUSTAL X shows that residues Gly43, Gly60, Pro65, Gly81, Gly137 and Gly140 are conserved in Cu, Zn-SODs and are responsible for the maintenance of the active-site geometry. It has been demonstrated that these residues are involved in maintaining the structure of the active site of Cu, Zn-SOD[24]. Cu which attracts the superoxide anion is positioned closely from Arg143 in spinach and yeast SOD[6, 13]. Similar observation was noted in AMSOD. It has been demonstrated that Arg143 attracts negatively charged species to the Cu active site channel and with Thr137, sterically excludes large nonsubstrate anions[25]. Small anion inhibitors such as cyanide, azide, and fluoride bind directly to the copper ion, however they come into the active site cavity and competitively inhibit the enzyme[26].

Table 2: Interaction in the form of salt bridges and hydrogen bonds between amino acid residues involved in coordination with metal ions in *A. marina* superoxide dismutase (amsod)

Residues interacting with Cu	Residues interacting with Zn
His45 (NE2)-(OD2) Asp123	Asp82(OD2)-(N) Gly71
His45(O and N)-(N and O) Val117	Asp82(O)-(NE) Arg78
His47 (ND1)-(O) Gly60	His79(N)-(OD2) Asp82
His62(ND1)-(OD1) Asp82	Asp123 (OD1)-(NE2) His70
His119(N)-(O) Gly43	Asp123 (OD2)-(NE2) His70
	His70(N)-(O) Lys134

Zinc is coordinated by ND1 side chain of His62, 70, 79 and OD1 of Asp82, with an approximate tetrahedral geometry. These histidines located in the loop region are conserved in all SODs and are involved in a salt bridge formation that stabilizes the protein (Figure 2).

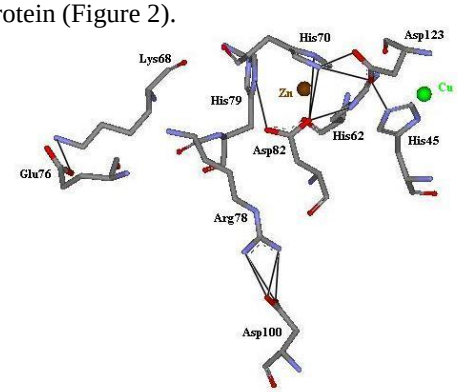

Figure 2: Coordination of catalytic residues with zinc. Salt bridge interactions of catalytic residues are also shown.

The interaction between these active site residues in the form of hydrogen bonds and salt bridges is outlined in Table 2. Crystallographic and spectroscopic studies demonstrate that His63 which is conserved in all Cu,Zn-SODs act as a bridging ligand between Cu and Zn ions in the cupric form of the enzyme[6, 9,13]. It is likely, therefore that His63 bridge is also found in AMSOD.

Electrostatic loop

In AMSOD, the residues predicted to be involved in the electrostatic substrate guidance and orientation are present in the coil region between 8 and 9 β-sheets as in case of other Cu,Zn-SODs[27]. These residues are positioned at 132-144 and are involved in the guidance of the substrate and in narrowing the channel used in substrate discrimination[28]. Leu132 and Thr135 are present at the rim of the active site channel in AMSOD. Main chain oxygen of Leu132 forms hydrogen-bonding network linking residues at Thr135, Thr136, and Gly137 (Figure 4a). Main chain nitrogen of Leu132 is hydrogen bonded to His130 while in case of SSOD such type of interaction was not found. It is assumed that Leu132 along with Thr135 may provide a possible route to SOD inhibitors or molecules of drug-like proportions to competitively fill this gap if having structurally specific potential. In addition, Gly128 and Gly129 are also conserved in SODs.

It has been demonstrated that when these residues are substituted by Asn and Arg respectively, they persuade changes in the conformation and charge distribution of the electrostatic loop that may have consequences for substrate encounter and local topography of the entrance to the catalytic site[27]. In our predicted mutated model of Gly128 → Asn and Gly129→Arg, Leu132 is hydrogen bonded to His130 and Asn128 is hydrogen bonded to His130 (Figure 4b). Accessibilities of Asn128 and Arg129 were also increased from 8 to 19Å and from 20.9 to 67.6Å respectively. Mutated Arg is more exposed to the surface of the protein as compared to original glycine residue. It is therefore likely that it will cause a change in the charge density of the protein surface and hence the interaction with other molecules might be affected.

Azide-bound model

The homology model of azide bound AMSOD (AMSODAZ) is structurally related to previously determined BSOD (1sxz) with RMSD of 0.32Å. The copper is coordinated with His43, His45, His60, His117 and azide with mean coordination distance of 2.63Å (Fig. 4). In AMSOD, the distances between

the His60 (NE2)-Cu, His60 (ND1)-Zn and His60 (NE2)-azide are 2.93Å, 2.68Å, and 2.57Å respectively. It has been demonstrated that His60 is present at an axial ligand position and easily dissociate from copper ion upon azide binding[6,9]. In AMSOD, His60 forms strong ionic bond with the azide anion as in case of BSOD. It is also observed that copper and distal nitrogen atom of azide are present near the guanidinium nitrogen of Arg140.

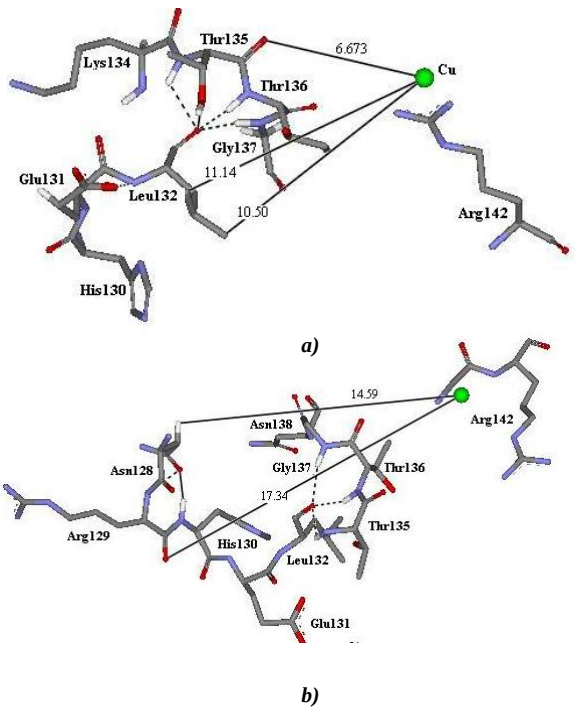

Figure 3: The Electrostatic Loop in *A. marina* superoxide dismutase (a) Hydrogen bonding network between residues Leu 132, Thr135, Thr136 and Gly137. Also shown are the distance between Cu-Leu132 and Cu-Thr135. (b) Predicted mutated model of Gly128 → Asn and Gly129 → Arg: No change was predicted in the hydrogen bonding pattern. Also shown are the distance between Cu-Asn128 and Cu-Arg129.

Thiocyanide-bound model

The 3D homology model of thiocyanate bound AMSOD (AMSODSCN) resembles that of previously determined structure of BSOD[9] (1sxs) with an RMSD of 0.33Å. At the active site, copper is coordinated with His62, His119 and nitrogen of thiocyanide as shown in Fig. 3b. The distance between His62 and thiocyanide (N) with copper is same while that between His119 and thiocyanide (N) with copper is 3.4Å and 2.63Å respectively**.**

It is therefore predicted that His62 is having the same coordination to copper and nitrogen of thiocyanide but His119 coordinate weakly with the thiocyanide because of the shift of 0.05Å upon binding while coordination with copper and zinc remains the same.

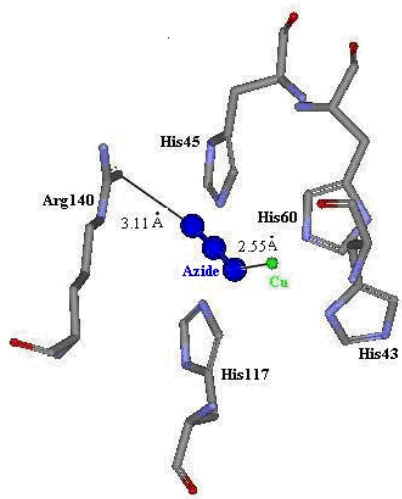

Figure 4: Metal binding sites in *A. marina* models bound with inhibitors: Coordination of Cu ion with catalytic histidines in Azide bound model. His117 is an axial ligand that otherwise does not interact with Cu in the model without the inhibitor.

Phosphate-bound model

The 3D homology model of phosphate bound AMSOD (AMSODPO4) is structurally similar to previously determined structure of YSOD with the RMSD of 0.38Å. It has been demonstrated that the positively charged amino acid residues present near the catalytic site are partially neutralized by interactions with anion at high ionic strength and play a significant role in the interaction of the protein with superoxide. These residues are responsible for the electrostatic guidance of superoxide to the active site[29]. It has been demonstrated that increasing ionic strength of phosphate causes decrease in the BSOD activity as well as its coordination for anion binding[30]. X-ray crystallographic study of BSOD showed that Arg-141, Lys120 and Lys-134 are found in the surrounding area of the catalytic site at a distance of 5, 12, and 13Å, respectively, away from the copper ion[29]. A similar prediction was made in the mutant 3D homology model of AMSOD; In Pro122 to Arg mutation, NE of Arg122 is coordinated to phosphate (O3, and O4) at distances of 3.30 and 2.77Å, respectively, while NH2 is coordinated with O3 of phosphate with a distance of 2.41Å while no coordination was observed in case of Pro (Figure 5a-b). In case of YSOD, NH1 and NH2 of Arg43 are coordinated with O4 and O3 of phosphate with distances of 2.91 and 2.65Å respectively. Arg142 which is conserved in all SODs plays a key role in catalysis by providing an electric gradient to attract the negatively charged O2 substrate. Cu-Zn has more affinity to phosphate as compared to azide or cyanide as reduced binding

affinity of the later was demonstrated in BSOD[30]. The coordination of catalytic residues with Cu and Zn remained the same (Figure 5c).

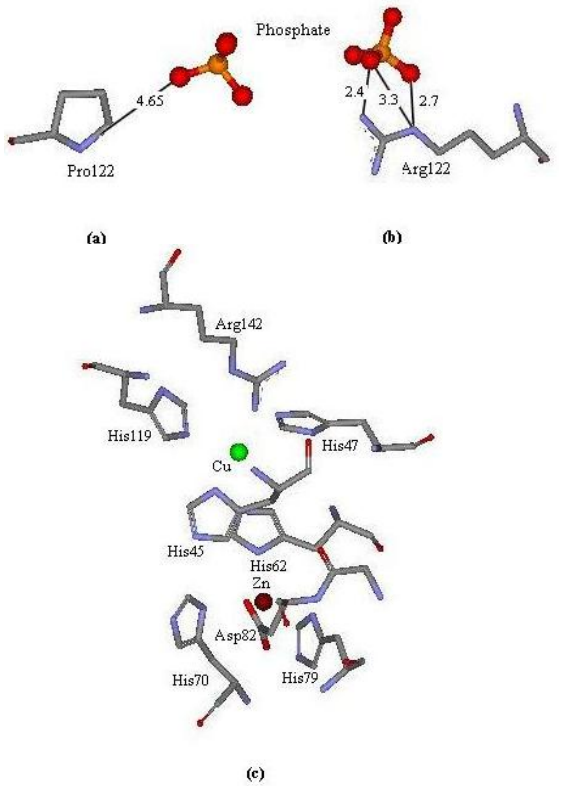

Figure 5: Phosphate bound models of AMSOD: (a) Original model with weak coordination between Pro122 and phosphate; (b) Mutant Arg122 shows stronger coordination with phosphate; (c) Conserved coordination between Cu and Zn ions with catalytic histidines and aspartic acid.

Nitrite-bound model

The homology model of nitrite bound AMSOD mutant (AMSODNO) is structurally related to previously determined BSOD (1sda) with RMSD of 0.28Å. However, significant changes were observed in the coordinating site of metals in the catalytic site. It was observed that the difference in RMSD of the original model of AMSOD and that of the AMSODNO mutant is at the level of 0.83Å between backbone atoms. Experiments have shown that Cu,Zn-SOD enhances tyrosine nitration of 4-hydroxyphenylacetic acid[31]. Therefore kinetics of tyrosine nitration in the presence of Cu,Zn-SOD studies have shown that Cu,Zn-SOD is a better effector for the PN-mediated nitration due to its ability to bind PN tighter and the PN-Cu,Zn-SOD complex can nitrate the peptide with a faster rate[32]. To determine the effect of nitration on the activity of AMSOD, we modeled mutants in which Pro108 and His109 were mutated to Asp and Tyr respectively (Figure 6a). In the mutated model, OD2 of Asp108 coordinates with O1, N, and O2 atoms of nitrite with distances of 2.32Å, 2.64Å, and 2.45Å, respectively, (Figure 6b). Phenolic hydroxyl group of Tyr109 is coordinated with N and O2 with distances of 3.05Å and 3.7Å respectively. In AMSOD, Asp82 is found as axial ligand; the side chain atoms, OD1 and OD2 are coordinated with Zn with distances of 2.58Å and 2.82Å respectively upon nitration. The remaining interaction of active site residues with copper and zinc is relatively similar.

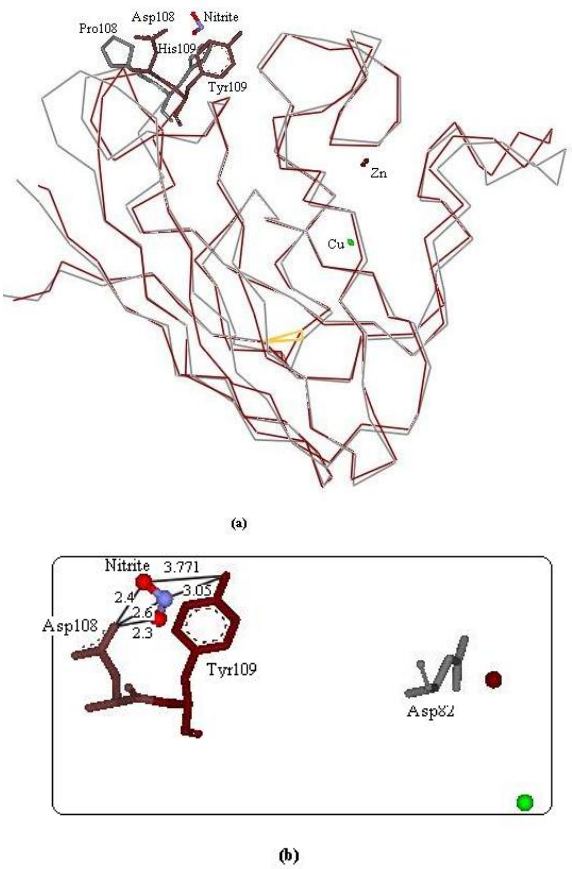

Figure 6: Nitrite bound models of AMSOD: (a) Original (grey) and mutant (brown) models of AMSOD are superposed with an RMSD of 0.8Å; (b) Asp108 and Tyr109 are seen coordinating with nitrite.

CONCLUSION

Plant cells have to survive constantly in the presence of various reactive oxygen radicals. They have evolved a complex series of enzymatic and non-enzymatic antioxidant protective mechanisms. It is well-established that the metallo-enzyme, superoxide dismutase (SOD) plays a vital role in protecting aerobic organisms against oxidative

damage and catalyze the dismutation of superoxide radicals to H_2O_2 and molecular oxygen. Mangroves that are salt-tolerant plants are better protected from oxidative damage under salt stress. The present study illustrates the prediction of structural aspects of superoxide dismutase from Mangrove specie, *A. marina*. The structural features of AMSOD were correlated with the functional aspects of the enzyme and thus its relation in coping with oxidative damage. The present study also attempts at the prediction of three-dimensional structures of AMSOD along with the specific inhibitors, azide, phosphate, thiocyanide and nitrite. Despite sequence variations, the inhibitor-enzyme interactions were quite similar. However, a few structural changes were predicted. The distances between copper and azide showed weak coordination. The copper is coordinated with His43, His45, His60, His117 and azide with mean coordination distance of 2.63Å. In case of thiocyanide, His62 is having the same coordination to copper and nitrogen of thiocyanide but His119 coordinate weakly with the thiocyanide. Mutations at crucial sites and a few structural changes were observed emphasizing the role of these residues in enzyme function.

REFERENCES

1. Vinocur B and Altman A. Recent advances in engineering plant tolerance to abiotic stress: achievements and limitations. *Curr. Opinion Biotech*., 2005; 16: 123-132.
2. Wuerges J, Lee JW, Yim YI, Yim HS, Kang SO and Djinovic CK. Crystal structure of nickel-containing superoxide dismutase reveals another type of active site. *Proc. Natl. Acad. Sci. USA*, 2004; 101: 8569-8574.
3. Barkasdjieva NT, Chrostov KN and Christina KN. Effect of calcium and zinc on the acivity and thermostability of superoxide dismuatse. *Biol. Plant*, 2000; 43: 73-78.
4. Navari-Izzo F, Quartacci MF, Pinzino C, Vecchia FD, and Sgherri CLM. Thylakoid-bound and stromal antioxidative enzymes in wheat treated with excess copper. *Physiologia Plantarum*, 1998; 104: 630-638.
5. Ogawa K, Kanematsu S and Asada K. Generation of superoxide anion and localization of CuZn-superoxide dismutase in the vascular tissue of spinach hypocotyls: their association with lignification. *Plant Cell Physiol.*, 1997; 38: 1118-1126.
6. Hart PJ, Balbirnie MM, Ogihara NL, Nersissian AM, Weiss MS, Valentine JS and Eisenberg D. A structure-based mechanism for copper-zinc superoxide dismutase. *Biochemistry*, 1999; 38: 2167-2178.
7. Takemura T, Hanagata N, Sugihara K, Shigeyuki B, Karube I and Dubinsky Z. Physiological and biochemical responses to salt stress in the mangrove, *Bruguiera gymnorrhiza*. *Aquat. Bot.*, 2000; 68: 15-28.
8. Arnesano F, Banci L, Bertini I, Martinelli M, Furukawa Y and O'Halloran TV. The unusually stable quaternary structure of human Cu, Zn-superoxide dismutase 1 is controlled by both metal occupancy and disulfide status. *J. Biol. Chem.*, 2004; 279: 47998-8003.
9. Ferraroni M, Rypniewski WR, Bruni B, Orioli P and Mangani S. Crystallographic determination of reduced bovine superoxide dismutase at pH 5.0 and of anion binding to its active site. *J. Biol. Inorg.Chem.*, 1998; 3: 411-422.
10. Bairoch A and Apweiler R. The SWISS-PROT protein sequence database and its supplement TrEMBL. *Nucleic Acids Res.*, 2000; 28: 45-48.
11. Altschul SF, Madden TL, Schaffer AA, Zhang J, Zhang Z, Miller W, and Lipman DJ. Gapped BLAST and PSI-BLAST: a new generation of protein database search programs. *Nucleic Acids Res.*, 1997; 25: 3389-3402.
12. Berman HM, Battistuz T, Bhat TN, Bluhm WF, Bourne PE, Burkhardt K, Feng Z, Gilliland GL, Iype L, Jain S, Fagan P, Marvin J, Padilla D, Ravichandran V, Schneider B, Thanki N, Weissig H, Westbrook JD and Zardecki C. The Protein Data Bank. *Acta Crystallogr. D. Biol. Crystallogr.*, 2002; 58: 899-907.
13. Kitagawa Y, Tanaka N, Hata Y, Kusunoki M, Lee GP, Katsube Y, Asada K, Aibara S, and Morita Y. Three-dimensional structure of Cu,Zn-superoxide dismutase from spinach at 2.0 A resolution. *J. Biochem.*, 1991; 109: 477-485.
14. Sali A and Blundell TL. Comparative protein modelling by satisfaction of spatial restraints. *J. Mol. Biol.*, 1993; 234: 779-815.
15. Sali A. A Program for Protein Structure Modeling Release 9v3, 2008 [URL http:// Salilab. org/ modeler/]
16. Smith CD, Carson M, Van der Woerd M, Chen J, Ischiropoulos H and Beckman JS. Crystal structure of peroxynitrite-modified bovine Cu,Zn superoxide dismutase *Arch. Biochem. Biophys.*, 1992; 299: 350-355.
17. Hall LT, Sanchez RJ, Holloway SP, Zhu H, Stine JE, Lyons TJ, Demeler B, Schirf V, Hansen JC, Nersissian AM, Valentine JS and Hart PJ. *Biochemistry*, 2000; 39: 3611-3623.
18. Guex N, Peitsch MC. SWISS-MODEL and the Swiss-PdbViewer: An environment for comparative protein modeling. *Electrophoresis*, 1997; 18: 2714-2723.
19. http://accelrys.com/products/discovery-studio/
20. Laskowski RA, McAurthur MW, Moss DS and Thornton JM. PROCHECK: A program to check the stereochemical quality of protein structures. *J. Appl. Cryst.*, 1993; 26: 283-291.
21. Sippl MJ. Recognition of errors in three-dimensional structures of proteins. *Proteins*, 1993; 17: 355-362.
22. Wiederstein M and Sippl MJ ProSA-web: interactive web service for the recognition of errors in three-dimensional structures of proteins. *Nucleic Acids Res.*, 2007; 35 (Web Server issue): W407–W410.
23. Rodriguez R, Chinea G, Lopez N, Pons T and Vriend G. Homology modeling, model and software evaluation: three related resources. *Bioinformatics*, 1998; 14: 523-528.
24. Cardoso RM, Thayer MM, Lo M, DiDonato TP, Bruns CK, Getzoff ED and Tainer JA. Insights into Lou Gehrig's disease from the structure and instability of the A4V mutant of human Cu,Zn superoxide dismutase *J. Mol. Biol.*, 2002; 324: 247-256.
25. Bertini I, Mangani S and Viezzoli MS. Structure and properties of copper/zinc superoxide dismutases. In: *Advanced Inorganic Chemistry*, Ed. Sykes AG, Academic Press, San Diego, California. 1998; 127–250.
26. Rigo A, Stevanato R and Viglino P. Competitive inhibition of Cu, Zn superoxide dismutase by monovalent anions. *Biochem. Biophys. Res. Commun.*, 1977; 79: 776-783.
27. Cardoso RM, Silva CH, Ulian de Araujo AP, Tanaka T, Tanaka M and Garratt RC. Structure of the cytosolic Cu,Zn superoxide dismutase from Schistosoma mansoni. *Acta Crystallogr. D Biol. Crystallogr.*, 2004; 60: 1569-1578.

28. Getzoff ED, Cabelli DE, Fisher CL, Parge HE, Viezzoli MS, Banci L and Hallewell RA. Faster superoxide dismutase mutants designed by enhancing electrostatic guidance. *Nature,* 1992; 358: 347-351.
29. Tainer JA, Getzoff ED, Beem KM, Richardson JS and Richardson DC. Determination and analysis of the 2 A-structure of copper, zinc superoxide dismutase. *J. Mol. Biol.,* 1982; 160: 181-217.
30. Mota de Freitas D and Valentine JS. Phosphate is an inhibitor of copper-zinc superoxide dismutase. *Biochemistry,* 1984; 23: 2079-2082.
31. Beckman JS, Ischiropoulos H, Zhu L, Van derWoerd M, Smith C, Chen J, Harrison J, Martin JC and Tsai M. Kinetics of superoxide dismutase- and iron-catalyzed nitration of phenolics by peroxynitrite. *Arch. Biochem. Biophys.,* 1992; 298: 438-445.
32. Kong SK, Yim MB, Stadtman ER and Chock PB. Peroxynitrite disables the tyrosine phosphorylation regulatory mechanism: Lymphocyte-specific tyrosine kinase fails to phosphorylate nitrated cdc2 (6-20) NH2 peptide. *Proc. Natl. Acad. Sci. USA,* 1996; 93: 3377-3382.